OFFICE OF NAVAL RESEARCH
Contract N/N00014-91-J-1893
R&T Code 4132062

TECHNICAL REPORT NO. 8

Thermochemistry of Silicate Speciation in Aqueous Sodium Silicate Solutions: Ionization and Polymerization of Small Silicate Ion

by

J. Yang and A.V. McCormick
Dept. of Chemical Engineering & Materials Science
University of Minnesota
421 Washington Ave. SE
Minneapolis, MN 55455

July 12, 1993

REPORT DOCUMENTATION PAGE

1. AGENCY USE ONLY (Leave blank)	2. REPORT DATE	3. REPORT TYPE AND DATES COVERED
	7/12/93	Technical

4. TITLE AND SUBTITLE
Thermochemistry of Silicate Speciation in Aqueous Sodium Silicate Solutions: Ionization and Polymerization of Small Silicate Ions

5. FUNDING NUMBERS
N/N00014-91-J-1893

6. AUTHOR(S)
J. Yang and Alon McCormick

7. PERFORMING ORGANIZATION NAME(S) AND ADDRESS(ES)
Dept. of Chemical Engineering & Materials Science
University of Minnesota
421 Washington Ave., SE
Minneapolis, MN 55455

8. PERFORMING ORGANIZATION REPORT NUMBER

9. SPONSORING/MONITORING AGENCY NAME(S) AND ADDRESS(ES)
Office of Naval Research
800 N. Quincy Street
Arlington, VA 22217

10. SPONSORING/MONITORING AGENCY REPORT NUMBER

11. SUPPLEMENTARY NOTES
Submitted to J. Physical Chemistry

12a. DISTRIBUTION/AVAILABILITY STATEMENT
Reproduction in whole or in part is permitted for any purpose of the U.S. Government. This document has been approved for public release and sale; its distribution is unlimited.

12b. DISTRIBUTION CODE

13. ABSTRACT *(Maximum 200 words)*

The thermochemistry of simple silicate oligomers in aquesous sodium silicate solutions is rationalized by a model that qualitatively predicts equilibria among monomer, dimer, and trimer silicate structures. Unlike previous models, it incorporates the influence of both silicate bonding and ion-solvent interactions on the stability of the anions. Although semiempirical molecular orbital calculations indicate that silicate bonds become less stable as charge increases, ion-solvent interactions tend to stabilize highly charged and compact silicate oligomers. Furthermore, polymerization is favored by the formation of highly stable water molecules and by a decrease of charge repulsion within the silicate structures. Although MNDO calculations indicate that the linear structures are more stable than the cyclic structures, ion-solvent interactions tend to stabilize the cyclic structures. Polymerization of compact silicate oligomers is also favored by producing more water molecules. Implecations are summarized for larger silicate species.

14. SUBJECT TERMS	15. NUMBER OF PAGES
silicate, NMR, thermochemistry, solvatic, MNDO	42
	16. PRICE CODE

17. SECURITY CLASSIFICATION OF REPORT	18. SECURITY CLASSIFICATION OF THIS PAGE	19. SECURITY CLASSIFICATION OF ABSTRACT	20. LIMITATION OF ABSTRACT
unclassified	unclassified	unclassified	UL

Thermochemistry of Silicate Speciation in Aqueous Sodium Silicate Solutions: Ionization and Polymerization of Small Silicate Ions

Jianchong Yang and Alon McCormick, Dept. of Chemical Engineering and Materials Science, 421 Washington Ave., SE, Minneapolis, MN 55455

To be submitted to J. Phys. Chem.

Abstract

The thermochemistry of simple silicate oligomers in aqueous sodium silicate solutions is rationalized by a model that qualitatively predicts equilibria among monomer, dimer, and trimer silicate structures. Unlike previous models, it incorporates the influence of both silicate bonding and ion-solvent interactions on the stability of the anions. Although semiempirical molecular orbital calculations indicate that silicate bonds become less stable as charge increases, ion-solvent interactions tend to stabilize highly charged and compact silicate oligomers. Furthermore, polymerization is favored by the formation of highly stable water molecules and by a decrease of charge repulsion within the silicate structures. Although MNDO calculations indicate that the linear structures are more stable than the cyclic structures, ion-solvent interactions tend to stabilize the cyclic structures. Polymerization of compact silicate oligomers is also favored by producing more water molecules. Implications are summarized for larger silicate species.

1 Introduction

The crystal structure of a zeolite is highly dependent on the composition and temperature of the synthesis solution. Recent reviews of the historical development and mathematical models of zeolite synthesis emphasize that future successes in the design of well-controlled, continuous synthesis processes will depend on a detailed and quantitative understanding of the distribution of solution species. Whether zeolites are formed directly from dissolved precursor anions [1-3] or from rearrangement of the network of a precursor gel [4,5], the population of the various precursors must still become quantitatively understood if zeolite synthesis is to be engineered.

Using ^{29}Si NMR experiments, various workers have obtain quantitative distributions of silicon among more than 20 silicate structures [6-16]. It has been shown that the structure of these silicates influences the nature of aluminosilicates present during zeolite synthesis. For instance, increasing the silicate ratio of the initial silicate solution increases the proportion of aluminum present in aluminosilicate structures during zeolite synthesis [17].

However, without the aid of a physically meaningful model, NMR measurements alone will not be sufficient to fully characterize the solution during zeolite synthesis. ^{29}Si NMR spectra are relatively insensitive to the degree of ionization and to structure beyond the second coordination sphere. Several NMR peaks from even relatively simple solutions remain unassigned. Furthermore, it is difficult to collect NMR spectra at the high temperatures characteristic of hydrothermal synthesis [2,18]. Therefore we have sought a rigorous thermodynamic model to relate the concentration of various silicate species to the overall solution composition. Previous attempts to develop such a model have relied on empirical assumptions and so are unable to explain *why* specific species are present. Such insight is essential to construct models for more complex species.

Although silicate and aluminosilicate solutions of technical interest typically contain a wide range of oligomeric species, in this work we begin by analyzing simple silicate solutions in which the only possible species are monomers and dimers. In fact, even such simple solutions can have up to 12 different anions! Rationalizing the behavior of even monomers and dimers can yield a great deal of insight into the reasons for construction of larger oligomers.

Although several workers have characterized silicate solutions [6-14] and have even discussed possible reaction networks, few have addressed how to explain reaction thermodynamics. For instance, Guth and Caullet [19-23] have modeled the distribution of silicate anions with reasonable success, but a number of simplifications were used. For instance, the polymerization equilibrium constants were assumed to be independent of the nature of the polymer species. At a given Si site, the free energy of ionization was assumed to increase linearly for each successive ionization. Finally, for successive ionization occurring on neighboring Si sites, the free energy of ionization was assumed to follow an empirical algebraic form [23]. Although this model accurately accounts for the distribution of small anions in dilute alkaline solution, it does not accurately predict the distribution of larger species. Moreover, it fails to explain why specific silicate structures (e.g. certain rings and cages) are formed. This leads us to reexamine the simplifying assumptions that were made.

One weakness of the model may lie in the assumption that all siloxane bonds are equally stable. De Jong et al. [30], for example, have used molecular orbital calculations to show a strong dependence of the bond stability on the bond angle. Another weakness lies in the functionality assumed for the ionization equilibrium constants. As will be discussed below, experimental data that the free energy of ionization for successive ionization does not vary in a linear fashion.

In another effort, Sjöberg et al.[25,26], used ^{29}Si NMR to characterize silicate species in fairly complex alkaline silicate solutions and thereby to estimate a large number of equilibrium constants [27,28]. Although these constants reasonably reproduce some experimental results, only discrete degrees of ionization were assumed to be present for each silicate species in the solutions even though there is no *a priori* reason why an oligomer should not exhibit all of the possible degrees of ionization. It would be valuable to learn what species are actually viable, since as the size of oligomers increases, the number of possible species (and equilibrium constants) increases catastrophically.

We start by considering the simplest alkaline silicate system, which we can verify by NMR to have only monomers and dimers. Since the number of possible species is small (five monomers and seven dimers), the number of independent equilibrium constants is manageable as only eleven independent chemical reactions are possible. By first restricting our attention to these few reaction equilibrium constants rather than to literally thousands that would be needed for complex solutions, we both ensure accuracy and will be able to observe meaningful trends.

We can specify the eleven independent reactions among monomers and dimers according to the following scheme:

$$\begin{array}{l} M^0 \leftrightarrow M^{1-} \leftrightarrow M^{2-} \leftrightarrow M^{3-} \leftrightarrow M^{4-} \\ \uparrow\downarrow \\ D^0 \leftrightarrow D^{1-} \leftrightarrow D^{2-} \leftrightarrow D^{3-} \leftrightarrow D^{4-} \leftrightarrow D^{5-} \leftrightarrow D^{6-} \end{array}$$

where M^{i-} and D^{i-} represent monomeric and dimeric anions (balanced equations are shown in reactions 1-3 below). These reactions are depicted systematically, with polymerization and

ionization being considered separately so that meaningful trends can best become apparent. We do not suggest that this reaction scheme is necessarily kinetically meaningful, but it is the most insightful for thermodynamic equilibrium calculations.

First we extract ΔH, ΔS and ΔG data for monomers and dimers from previous work which we carefully select so as to avoid complications resulting from reactions among too many anions. We also demonstrate that this data is capable of predicting the concentration distribution of monomers and dimers detected directly with ^{29}Si NMR. Most importantly, though, we rationalize these thermochemical trends using both MNDO and ion-solvation theory.

2 Experiments and Calculations

2.1 ^{29}Si NMR

Sodium silicate solutions with a total silica concentration of 0.2 mol% and with silicate ratios (SiO_2 / Na_2O) ranging from 0.02 to 0.5 were prepared from high purity silica gel (Aldrich), sodium hydroxide (99.99% pellets from Aldrich) , and distilled and deionized water. ^{29}Si NMR experiments were performed at 298°K on a GE-500 spectrometer with a 10 mm sample tribe. A paramagnetic relaxation reagent ($Cr^{(III)}$) was added to all solutions to reduce the ^{29}Si spin lattice relaxation time to 1-2. The Cr^{III} concentration was low enough [8,9], though, that there was no significant change in the anion distribution. All chemical shifts use $Si(CH_3)_4$ as a reference. Spectra were recorded using 256 26 μs (≈90°) pulses with a pulse repetition time of 10s, a spectral width of 10 kHz, and a line broadening factor of 5 Hz.

2.2 MNDO calculations

In order to study the effects of silicate bond stability, calculations were performed using the MNDO Hamiltonian introduced by Dewar and others [29-32]. MNDO has recently been reparameterized for silicon, so it is useful for rationalizing thermochemical trends for silicates [33]. A number of fairly successful calculations have been carried out for molecules characterized by π bonding and/or partial ionic bonding such as SiO_2 and $SiCl_4$ [33]. Though the expected error in value of the heat of formation is about 33 kcal/mol silicon [32], the trends suggested by MNDO calculations of silicate anions should be meaningful.

It is important to bear in mind that the stability of solvated silicate anions is quite different from that of anions in vacuum. As an example of how important this proviso is, MNDO has been used to predict a stable pentacoordinate silicate structure [34] even though only tetrahedral structures are observed experimentally in aqueous solution. All results reported in this paper are for optimized structures constrained to tetrahedral silicon coordination.

3 Thermochemistry of monomers and dimers

3.1 NMR Measurements

In Figure 1, the spectra obtained for dilute solutions with increasing silicate ratio (decreasing pH value) show that the solutions contain only monomers and dimers. The distribution was determined by integrating the spectra and is shown in Figure 2 The dimer is first formed in significant concentration at a silicate ratio of 0.1, and thereafter it increases in concentration as the

silicate ratio increases. The test of whether thermochemical values from the literature are correct will lie in their ability to reasonably predict the value of R where dimerization begins.

3.2 Selection of Thermochemical Values

3.2.1 Ionization of Monomers

There is a great deal of discrepancy among reported monomer ionization constants [25,26,35-40]. Some workers [36] used silicate solutions which are too concentrated or at too low a pH to ensure that monomers are the only species present in solution. The interference of other reactions brings the thermochemical values into serious question. Other workers [25,26] used sufficiently dilute and basic solutions, but their calculation of ionization constants is based on the assumption that only a few of the five degrees of ionization are possible. However, Flint et al. [37] used very dilute solutions and all monomer anions were considered. Moreover, the free energies of ionization obtained by Flint agree with those reported by Mel'nik, Babushkin and Iler et al. [39-41]. Therefore, we have taken Flint's values as the most reliable.

The standard Gibbs free energy, ΔG_i^o for each successive ionization is shown in Fig.3a, where the reaction is of the type

$$Si(OH)_m Q_n^{n-}{}_{aq} + OH^-_{aq} = Si(OH)_{m-1} Q_{n+1}^{(n+1)-}{}_{aq} + H_2O_{aq} \qquad (1)$$

While successive ionization of the monomer becomes more difficult, this trend levels off at high charge. This trend runs contrary to the assumption made in previous models [19-23] that the free energy of ionization varies linearly with the degree of ionization.

Enthalpies of reaction have also been found from variable temperature investigations [40], and Figure 3b shows that the

enthalpy of successive ionization of the monomer goes through a minimum. The entropic contribution to the ionization of monomers can then be obtained. Figure 3c shows that the first ionization is strongly entropically favored, but subsequent ionizations are almost equally *opposed*. Notice that ionization becomes more difficult only because of the unfavorable entropy trend, but the free energy is modulated by the enthalpy trend.

3.2.2 Formation and Ionization of Dimers

Sjöberg [27,28] estimated formation free energies with the aid of both ^{29}Si NMR and conductimetric methods, and from these we can extract both dimerization and dimer ionization equilibrium constants corresponding to reactions 2 and 3.

$$2Si(OH)_{4_{aq}} = (HO)_3SiOSi(OH)_{3_{aq}} + H_2O_{aq} \qquad (2)$$

$$Si_2(OH)_{6-n}O_{n+1_{aq}}^{-n} + OH_{aq}^- = Si_2(OH)_{5-n}O_{n+2\ aq}^{(n+1)-} + H_2O_{aq} \qquad (3)$$

Thus we find from Sjöberg's data that the free energy of dimerization has a value of only -0.7 kcal/per mol Si. Figure 2-4 shows the free energy of successive ionization of the dimer. The dimer ionization trend is similar to that of monomers, but the dimer is more acidic than the monomer at low charge and then becomes less able to ionize at high charge.

Notice that that free energy of dimerization (2) is negligible compared to the free energy of the many various ionization reactions of types (1) and (3). This indicates that the distribution of monomers and dimers is governed primarily by the stability of the various ions and the activity of the hydroxide ion. Dimerization occurs only when the activity of the hydroxide anion is low enough that the hydroxide is no longer driven to ionize as many silanol groups as can only be provided by monomers. Therefore, it is clear that we need to

understand the ionization energy in great detail for various oligomers.

3.2.3 Confirmation of thermochemical values

In figure 5, we show the calculated composition at 298°K as a function of silicate ratio at a fixed SiO_2 concentration (0.2mol%) using the data from figures 2-4. It is assumed in these calculations that activity coefficients are weak functions of R in these dilute solutions. We observe reasonable agreement with experiment, but the concentration of dimers is underestimated. If we maintain the ionization constants, but increase the magnitude of ΔG of dimerization to that estimated from quartz solubility (-2.0 kcal/molSi [19]), agreement with experiment improves (Fig.5b).

Another possible improvement would be to estimate the effect of the silicate ratio on ion activities, but so long as the ionic strength of the solution remains low enough to rely on the extended Debye-Hückel theory, ion-ion interaction will not much affect the distribution of ions. At the concentration used, we expect activity corrections to be negligible at a silicate ratio as low as 0.5 (where the ionic strength of the solution is about 0.04M), but should become increasingly important at higher R.

4 Rationalization of Monomer and Dimer Thermochemistry

So far, we have only selected thermodynamic values for simple species from experiments and shown that they are consistent with NMR for dilute, very alkaline solutions. If larger species were present, many more thermochemical values would have to be specified, and their accuracy and precision would be in doubt without some understanding of the behavior of even the simplest ammonia. For this reason, we seek to rationalize the trends in ΔG, ΔH, and ΔS using MNDO and solvation theory.

4.1 MNDO Calculation of Ionization Thermochemistry

Figure 6 shows the heat of formation of linear silicate anions in vacuum as calculated by MNDO. The values are reported per mol Si rather than per mol anion because we wish to compare the stability of a given Si unit in each environment. Each anion becomes less stable with increasing charge largely because ionization increases the Coulombic repulsion energy between atomic centers.

Ideally we want to calculate the ionization enthalpy of monomers in aqueous state, (reaction (1)) but with MNDO we can only obtain results in vacuum. Estimated enthalpies of ionization, calculated from data in Fig. 6, are shown in Figure 7 for the following type of ionization reactions,

$$Si(OH)_mQ^{n-}_{n\,vac} + OH^-_{aq} = Si(OH)_{m-1}Q^{(n+1)-}_{n+1\,vac} + H_2O_{aq} \qquad (4)$$

where subscript *vac* indicates that silicate species is in vacuum state. The reference state will be corrected in the next section.

Though MNDO correctly predicts that the dimer is slightly more acidic for the first ionization, it incorrectly indicates that the dimer is more acidic at high charge and that each subsequent ionization would have a more positive enthalpy. This trend conflicts with experimental observations (cf. Fig.3). This discrepancy, then, suggests that the interaction with solvent plays an important role in stability, so in the following section we consider how to estimate the energy of ion-solvent interactions.

4.2 Ion-solvent Interactions

To study solvation effects, the extended Born model of ion-solvent interaction is used [42]:

$$\Delta H_{I\text{-}H_2O} \propto -\frac{N_A n z_i e_o \mu_W}{(r_i + r_W)^2} - \frac{N_A n z_i e_o p_W}{(r_i + r_W)^3}$$

$$- \frac{N_A (z_i e_o)^2}{2(r_i + 2r_W)} \times \left[1 - \frac{1}{\varepsilon_W} - \frac{T}{\varepsilon_W^2} \frac{\partial \varepsilon_W}{\partial T} \right],$$

where

$\Delta H_{I\text{-}H_2O}$	:	contribution to heat of formation due to ion solvent interaction
r_i, r_s	:	radius of ion and solvent molecules, respectively
N_A	:	Avogadro number
z_i	:	charge number of the ion
μ_s	:	dipole moment of solvent molecules
n	:	solvation number of the ion
p_W	:	quadrupole moment of water

The first term arises from the interaction between the ion and the dipoles of water molecules, the second term from the ion water-quadrupole interaction, and the last term (the Born contribution) from the work of transferring an ion from vacuum into a continuous medium with a dielectric constant ε_W. It should be noted that even the extended Born model is at best semi-quantitative when applied to complex silicate ions in aqueous solutions. Our current aim is limited to qualitatively rationalizing the thermochemical properties of the simplest silicates.

As a first approximation we estimate the silicate anion radius as the average distance from the center of a silicate structure to oxygen atoms in the end groups of the structure. Physically, this means that we assume that the negative charge on the anion can be treated as if it resides at the center of mass of the anion. The number of solvating waters is initially assumed to equal the charge

of the anion. In appendix A we discuss more realistic assumptions. The partial derivative in the third term is negligibly small for a dilute aqueous solution at 298°K, so it is neglected.

The contribution of the various ion-solvent interactions is shown in Table 1. Each contribution behaves in a qualitatively similar way, though the Born term grows more quickly than other terms. The total enthalpy of successive ionization of monomers and dimers including contributions both from MNDO calculations and ion-solvent calculations are shown in Fig. 8. The trend for the dimer is now qualitatively similar to the experimental trend in Fig.3b; subsequent ionization becomes more enthalpically favorable and then reverses at high charge. This is the consequence of competition between unfavorable anion destabilization (MNDO prediction) and favorable ion-solvent interactions. However, two problems remain: 1) this calculation predicts that ionization of the monomer becomes increasingly favorable <u>without</u> reversing, which conflicts with the experimental trend (Fig. 3b), and 2) larger silicates are more difficult to ionize than smaller silicates, which is also incorrect.

The experimentally derived values of the entropy of ionization (Fig. 3c) reveals clues as to how to improve the calculation of the ion-solvent energy. The monomer ionization trend shows that the third ionization introduces no more order to surrounding water molecules than does the second ionization. We deduce that ΔS is governed by two opposing trends:

1) Each ionization consumes a hydroxide anion and produces a water molecule, leading to a favorable entropy change of 19.3 cal/K.mol anion (obtained from standard values of H_2O_{aq} and OH^-_{aq}). This entropy contribution is constant for each successive ionization reaction.
2) Strong ion-solvent interactions, on the other hand, cause water molecules to be ordered in the solvation sphere of the anion. Since each ionization produces a more highly charged anion, this more charged ion sphere interacts more strongly with surrounding water

molecules, causing the water molecules to become more ordered. For this reason, each ionization tends to be entropically disfavored.

Apparently, though, the singly charged monomer is much less able to order water molecules than the hydroxide anion (Fig.3c), whereas multiply charged anions order water better then does the hydroxide anion. The organization of water molecules around a charged group should not be appreciably different for differently sized silicates, so we expect that the entropic behavior of ionization of dimer to follow the same trend as the monomer.

Fig. 3b also indicates that the highly charged monomer interacts no more strongly with water molecules than does the doubly charged monomer, so simply increasing the solvation number of a monomer in proportion to the charge number provides, of course, a poor model. In fact, only a few water molecules closely surround the monomer, whereas other water molecules must interact from a greater distance. Because the ion-solvent interaction energy falls off rapidly with separation, the increase of the monomer charge will not *proportionally* increase the degree of ion-water interaction. Moreover, the extended Born model treats an ion as a structureless sphere; this is a very crude assumption, since for a large structure (e.g. a linear trimer or tetramer), it is more reasonable to assume that a water molecule interacts with <u>one</u> charged silicon tetrahedron in the structure rather than with the whole structure. Details are discussed in appendix A, where we illustrate that ion-solvent interaction for various silicate structures is strongly model dependent. The current model fails to quantitatively predict the ionization trends mainly because it has few parameters to model such a complex interaction. However, it is clear now that the stability of silciate anions arises from a *balance* of bonding versus ion-solvent interactions.

5 Rationalization of Linear and Cyclic Trimer Thermochemistry

As the solution becomes more concentrated and less alkaline, cyclic silicate species are formed in preference to linear species.[7-11] Figure 9 illustrates MNDO calculations of the enthalpy of polymerization of the following type:

$$n\ Si(OH)_{4_{vac}} \Leftrightarrow Si_nO_{n-1}(OH)_{2n+2_{vac}}(Linear) + (n-1)H_2O_{aq} \qquad (5)$$

and shows that polymerization is generally favorable. According to the extended Born model, ion-solvent interactions should not influence these trends, since for now we are considering polymerization of only uncharged species, but more subtle ion-solvent interactions (such as dispersion forces etc.) are neglected here. Polymerization is favored mainly because it produces water molecules, and polymerization of larger linear oligomers doesn't become more favorable because the silicate bond becomes less stable for a larger structures. Polymerization of cyclic structures are more favored over the linear structures, because they produce more water molecules. This helps to explain why experiment shows that linear polymerization is limited in solution [6-12].

While *uncharged* cyclic structures are favored over *uncharged* linear structures, the energy of ionization is much larger than that of polymerization, so it is not yet clear why cyclic anions are favored over linear anions. MNDO calculations of the enthalpy of ionization for linear and cyclic trimers indicate that the linear trimer ionizes more easily than the cyclic trimer [Fig. 10]. By assuming that the entropic contribution to ionization is similar for both linear and cyclic trimer, we would come to the experimentally incorrect conclusion that the linear silicate oligomers should be favored. Therefore, we must again consider ion-solvent interactions.

Using the same assumptions as used for Table 1, one can show that as degree of ionization increases, the stability of a cyclic trimer can increase more rapidly than the linear trimer (Fig. 11), and the cyclic trimer is better able to ionize in solutions (Fig. 12). Cyclic

silicate oligomers ionize more easily because the ion size is smaller than for linear structures. The Born energy of ion-solvent interaction causes it to become more stable at a faster rate than in the linear anion as charge of structure accumulates.

6 Conclusions

Independently derived thermodynamical values accurately predict speciation of monomers and dimers but do not follow the simple trends that have been assumed in previous modeling studies. We found that MNDO alone could not predict the trend in ionization enthalpy, but inclusion of ion solvent interaction explains these trends qualitatively. We are still limited by the crudeness of the ion solvent model, but we demonstrate that the experimental trends result from the competition between bonding and ion solvent contribution.

The trends revealed in this study are consistent with data reported by other workers, but they reveal more physical insight regarding silicate speciation. Four general rules are obtained:

1) Each subsequent ionization of a silicate species in solution grows more difficult in a complex fashion that represents the interplay of three influences:
   a) the ordering of waters of hydration (producing a regular and predictable ΔS trend),
   b) destabilization of the molecules as charge increases (which can be predicted with MNDO calculations), and
   c) favorable energetic interactions between the ion and solvent (which can be qualitatively predicted by judicious use of extended Born theory).
2) Ionization is enthalpically more favorable for larger silicate species when they are only slightly charged, but it becomes more difficult then for a small species as they become more highly charged.

3) Ionization of cyclic species is more favorable than the correspond linear species due to shorter range stronger ion-solvent interactions.
4) Polymerization is favorable because it produces highly stable water molecules, and polymerization of cyclic silicates is more favorable than the linear silicates because it produces more water molecules. The thermochemistry of small silicates, though, seem to be governed by both bonding stability and ion-solvent interactions.

Ion-solvent interactions are very difficult to model. Future success in predicting the behavior of silicate and aluminosilicate species will rely on modeling ion-solvent interactions.

Acknowledgements

This work was supported by grants from the National Science Foundation (CTS-9058387-01), the Office of Naval Research, and the Dow Chemical Company. The authors are grateful for discussions with Juan Garces of the Dow Chemical Company.

Appendix A

The extended Born model fails to quantitatively predict ionization trends for linear silicate oligomers because of the difficulty in identifying the number of solvation water molecules of a silicate anion and because of the crude treatment of a silicate anion as a charged sphere. To address these problems, we can modify the calculations in the following way:

1) a water molecule interacts only with one charged silicate tetrahedron, where the radius of the tetrahedron is the average of the four Si-O bonds,

2) the number of water molecules that interact with a specific silicate tetrahedron increases initially in proportion to the charge of that tetrahedron, but,

3) when the charge grows beyond 2, the solvation number increases more slowly (Fig.13),

4) the charge distribution on the dimer is optimized to provide minimum $\Delta H_{I\text{-}H_2O}$ (so that one end is first charged up to *3*-, then the other end charged to *k*-).

The modified calculations (Fig. 14) show that better agreement with experiment can be achieved. Fig. 14 also indicates that large silicates ionize more easily than the smaller silicates when they carry low charge, but large silicates are harder to ionize than the smaller silicate when highly charged.

However, using the modified ion-solvent interaction model derived above, the calculated values for the enthalpy of ionization do not show that the cyclic trimer ionizes more easily than the linear trimer [Fig. 15]. In the modified model, we made an assumption that a water molecule interacts with only one specific charged Si group and neglected the interaction with other Si groups. But we must count on this interaction when we want to compare ionization trends of two structurally different species. This is illustrated in Figure 16. As in the illustration of Fig. 16a, a water molecule can have strong

interactions with two Si groups in an equally charged linear tetramer. However, in Fig. 16b, a water molecule can strongly interact with four charged Si groups simultaneously. So, ion-solvent interaction of cyclic structure is stronger than for the correspond linear structure.

Inclusion of such complex interaction in the ion-solvent interaction model overstretches the extended Born model.

References

[1] Barrer, R. M., *Zeolite 1*, **1981**, 131.

[2] Barrer, R. M., *The Hydrothermal Chemistry of Zeolites*, Academic Press, London, **1983**.

[3] Ueda, S., Kageyama, N., and Koizumi, M., in " *Proc. 6th Int'l. Zeol. Conf.* " (A. Bisio and D. H. Olson, eds.), Butterworth, Guildford, U. K. **1984**, p. 905.

[4] Flanigen, E. M., in " *Proc. 5th Int'l. Zeol. Conf.* ", (L. V. C. Rees, ed.), Heyden, London, **1980**, p. 760.

[5] McNicol, B. D., Pott, G. T., and Loos, K. R., *J. Phys. Chem.* 76, **1972**, 3388.

[6] Harris, R.K.; Neman, R.H., *J.Chem.Soc. Faraday Trans.* 2, **1977**, 73, 1204.

[7] Engelhardt, Von G.; Hoebbel, D.; Tarmak, M.; Samoson, A.; Lippmaa, E., *Z. anong. allg. Chen.* 484, **1982**, 22-32.

[8] Harris, R.K.; Knight, C.T.G., *J.Chem. Soc. Faraday Trans.* 2, 79, **1983**, 1525-1538.

[9] Harris, R.K., Knight, C.T.G., *J.Chem. Soc. Faraday Trans.* 2, 79, **1983**, 1539-1561

[10] Harris, R.K.; O'Connor, M.J.; Curzon, E.H.; Howarth, O.W., *J. Magn. Reson.*, 57, **1984**, 115.

[11] McCormick, A.V., Bell, A.T.; Radke, C.J., *Zeolite* 7, **1987**, 183.

[12] Knight, C.T., *J. Chem. Soc. Dalton Trans.*, **1988**, 1457.

[13] Kinrade, S.D.; Swaddle, T.W., *Inorg. Chem.* **1988**, 27, 4253

[14] Kinrade, S.D.; Swaddle, T.W., *Inorg. Chem.* **1988**, 27, 4259

[15] McCormick, A.V.; Bell, A.T.; *Catal. Rev.-Sci.Eng.*, 31(1&2), **1989**, 97-127.

[16] Bell, A.T., *Zeolite Synthesis-ACS Symp. Ser.*, **1989**, 66-82

[17] Mortlock, R.F.; Bell, A.T.; Chakraborty, A.K., and Radke, C.J.; *J. Phys. Chem.* **1991**, 95, 4501-4505

[18] Vaughan, D.E.W., *Chem. Eng. Prog.* 84(No.2), **1988**, 25-31.

[19] Guth, J.L.; Caullet, P., Bull. *Soc. Chim.*, Fr., **1974**, 1758.

[20] Guth, J.L.; Caullet, P., Bull. *Soc. Chim., Fr.*, **1974**, 2363.
[21] Guth, J.L.; Caullet, P., *Chem. Soc. France*, **1980.**
[22] Guth, J.L.; Caullet, P., *Studies in Surface Science and Catalysis*, 24, Elsevier, Amsterdam,**1985**, 183.
[23] Caullet, P.; Guth, J.L., *Zeolite Synthesis-ACS Symp. Ser.*, **1989**, 83-97.
[24] De Jong, B.H.W.S.; Brown, G.E., *Geochimica Acta* Vol.44, **1980**, pp.491-511
[25] Lagerström, G., *Acta Chem. Scand.*, 13, **1959**, 722-736.
[26] Ingri, N., *Acta Chem. Scand.*, 13, **1959**, 758-775.
[27] Sjöberg, Staffan, Öhman, Lars-Olof; Ingri, Nils, *Acta Chemica Scand.* A39, **1985**, 93-107.
[28] Sjöberg, Staffan, Öhman, Lars-Olof, *J.Chem.Soc., Faraday Trans. I*, 82, **1986**, 3635-3646.
[29] Dewar, M.J.S.; Thiel, W., *J. Am. Chem. Soc.* 99, **1977**, 4907.
[30] Dewar, M.J.S.; Rzepa, H.S., *J. Am. Chem. Soc.*, 100, **1978**, 784.
[31] Clarke, T., *A Handbook of Computational Chemistry*, Wiley, NY, **1985**.
[32] Stewart, J.J.P., *J. Computer-aided Mol. Des.*, 4, No.1, **1990**.
[33] Dewar, M.J.S.; Friedheim, J.; Grady, G.L.; Healy, H.F.; Stewart, J.J.P., *Organometallics*, 5, **1986**, 375-379.
[34] Davis, L.P.; Burggraf, L.W., *Ultrastructure Processing of Advanced Ceramics*, (Ed. Mackenzie, J.D.; Ulrich, D.R.), Wiley-Interscience, NY, **1988**, 367-378.
[35] Perry, R.H.; Green, D., *Perry's Chem. Eng. Handbook*, **1984**, 4-78.
[36] Harman, R.W., *J. Phys. Chem.* 31, **1927**, 617.
[37] Flint, E.P.; Wells, L.S., *Bur. Scand. J. Res.*, 12, **1934**, 751.
[38] *J. Phys. Chem. Ref. Data.*, Vol.11, **1982**.
[39] Mel'nik, *Thermodynamic Constants for Analyzing the Conditions of Formation of Iron Ores*, Naukova, Dumka, **1972**
[40] Babushkin, V.I.;Matveyev, G.M.; Mchelov, O.P., *Thermodynamics of Silicates*, Springer-Verlag, NY, **1985.**
[41] Iler, R.K., *The Chemistry of Silica*, Wiley, **1979**.
[42] Bockris, J. O'M.; Reddy, A.K.N., Modern Electrochemistry, Plenum, NY, **1977**.

Table 1 Sample calculation of ion-solvent interaction enthalpy for monomers (kcal/mol Si)

z_i	r_i (Å)	$\Delta H_{ion\text{-}dipole}$	$\Delta H_{ion\text{-}quadrupole}$	ΔH_{Born}	$\Delta H_{I\text{-}H_2O}$
0	1.65	0.0	0.0	0.0	0.0
1	1.66	-18.2	-13.3	-44.6	-76.1
2	1.68	-72.0	-52.5	-178	-302
3	1.69	-160	-116	-398	-674
4	1.71	-281	-202	-705	-1190

Figure Captions

1 ^{29}Si NMR spectra of sodium silicate solutions at a constant concentration of 0.2mol% SiO_2. The chemical shift reference is the monomer.

2 Measured distribution of monomer and dimer in sodium silicate solutions at a fixed silicate concentration of 0.2mol%.

3 a ΔG of successive ionization of monomers at 298°K: (reactive 1). Data are calculated from Flint [37], Mel'nik [39] and Babushkin et al [40]. Error bars reflect scatter of value reported by various workers.

3 b ΔH of successive ionization of monomers (reaction 1). Data calculated from Babushkin[40].

3c ΔS of successive ionization of monomers (reaction 1) using data from Babushkin[40].

4 ΔG of ionization for the successive ionization of dimers (reaction 3) obtained from data of Sjöberg et al [27,28].

5 Comparison of calculated with experimental compositions for silicate solutions of constant silicate concentration of 0.2mol%. (5a) ΔG_d=-0.7 kcal/mol Si; (5b) ΔG_d=-2.0 kcal/mol Si.

6 Enthalpy of formation from elements in their standard states for monomer and dimer, obtained from MNDO calculation.

7 Enthalpy of ionization in vacuum (reaction 4) predicted by MNDO calculation.

8 Successive ionization of monomer, dimer in solution, calculated by conbining MNDO and extended Born theory.

9 Enthalpy of polymerization from uncharged monomers to uncharged dimer, linear trimer and linear tetramer in vacuum.

10 Enthalpy of ionizations of linear trimer, cyclic trimer using MNDO calculation.

11 Enthalpy of formation for isolated (MNDO calculation only) and solvated (MNDO + ion-solvent interaction) linear and cyclic trimers.

12 Enthalpy of ionization for the linear and cyclic trimer in solutions.

13 Modified correlation between number of solvation water around a specific Si-tetrahedron and charge on the Si-tetrahedron.

14 Successive ionization of monomer, dimer in solution, calculated by MNDO and a *modified* extended Born theory.

15 Enthalpy of ionization for the successive ionization of linear and cyclic trimer in solutions by MNDO and a *modified* extended Born theory.

16a A water molecule interacting with a charged linear tetramer ($Si_4O_7(OH)_8^{4-}$)

16b A water molecule interacting with a charged cyclic tetramer ($Si_4O_8(OH)_4^{4-}$)

Figure

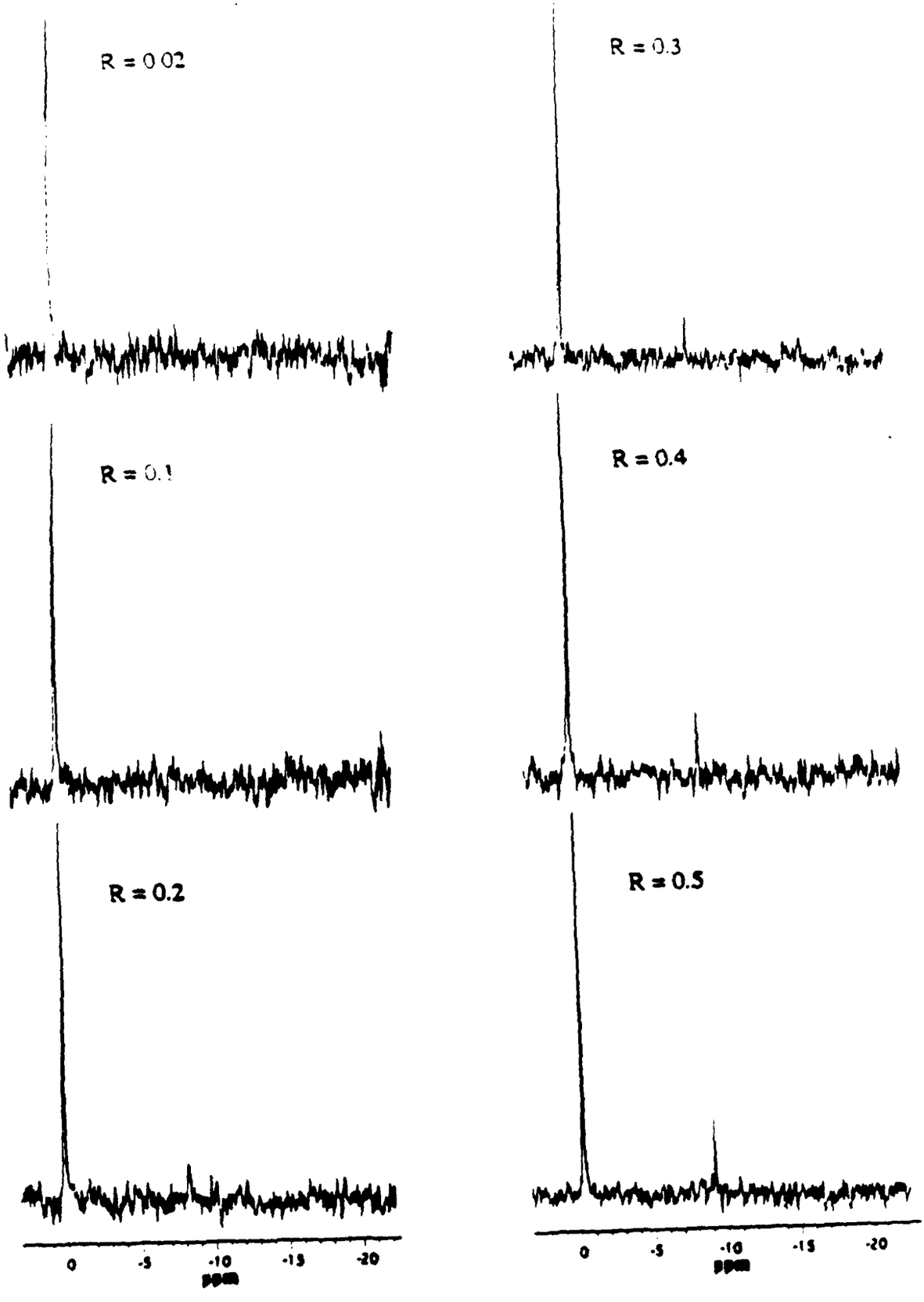

Figure 2

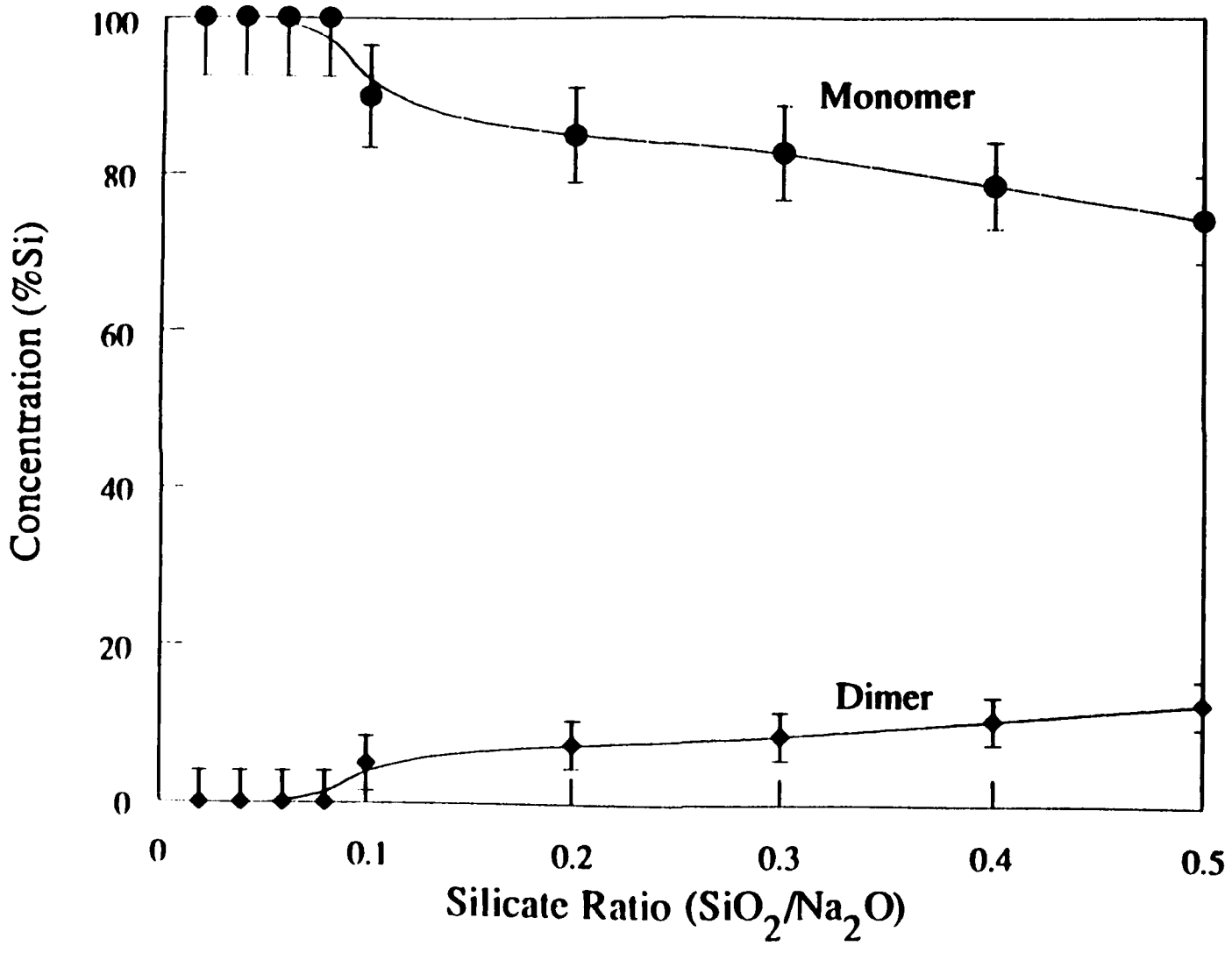
100
80
60
40
20
0
Concentration (%Si)
Monomer
Dimer
0
0.1
0.2
0.3
0.4
0.5
Silicate Ratio (SiO_2/Na_2O)

Figure 3a

a)

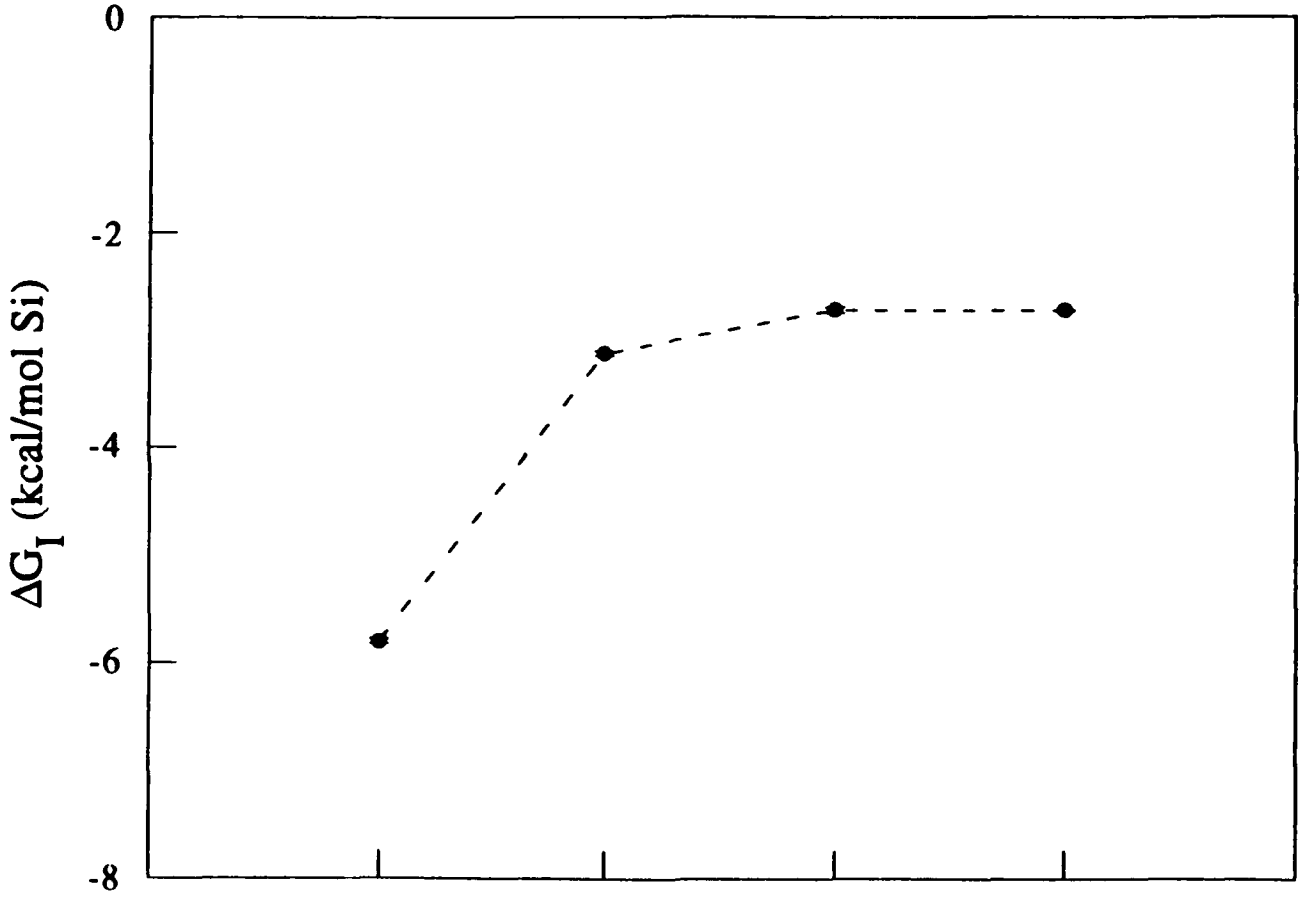

Figure 3b

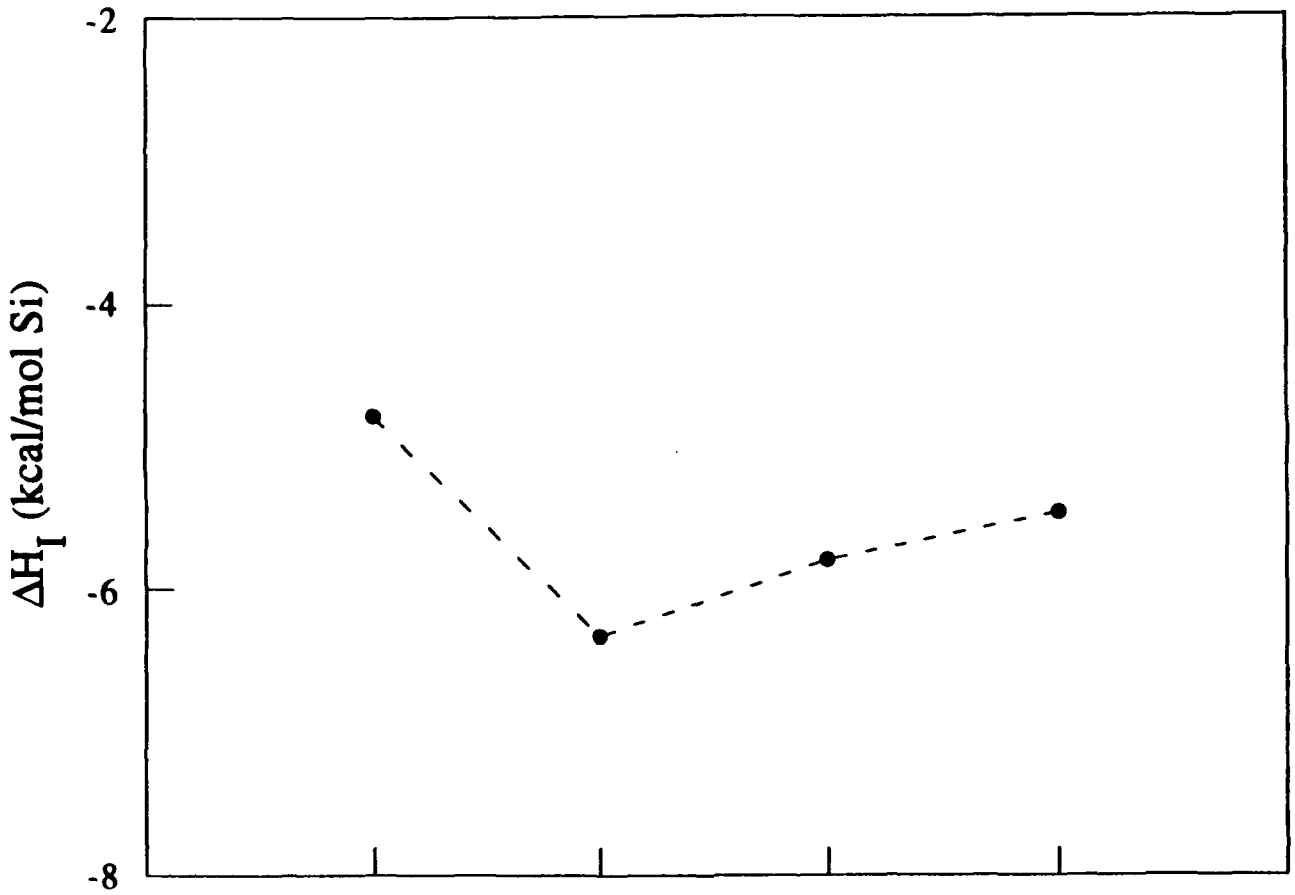

Figure 3c

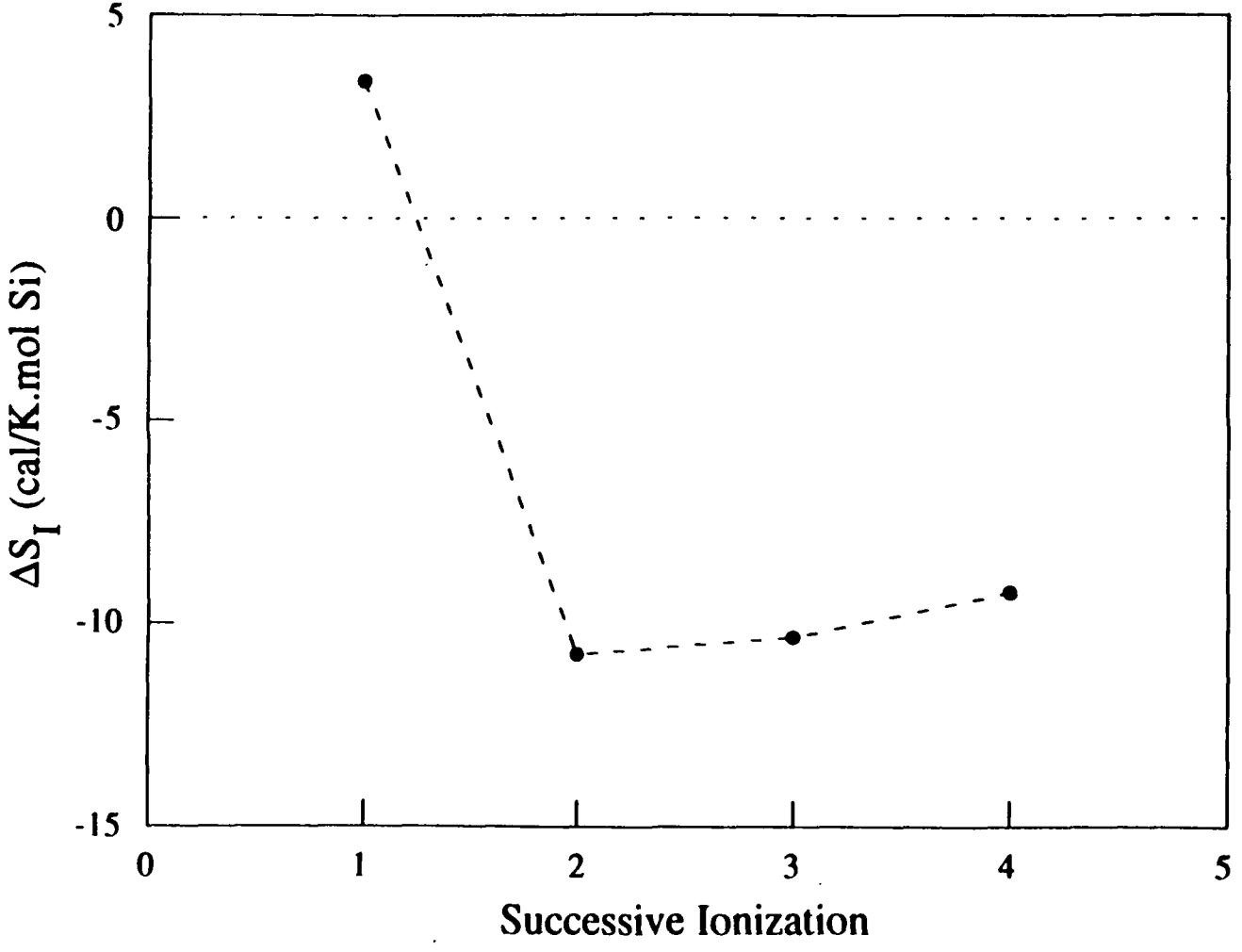

Figure 4

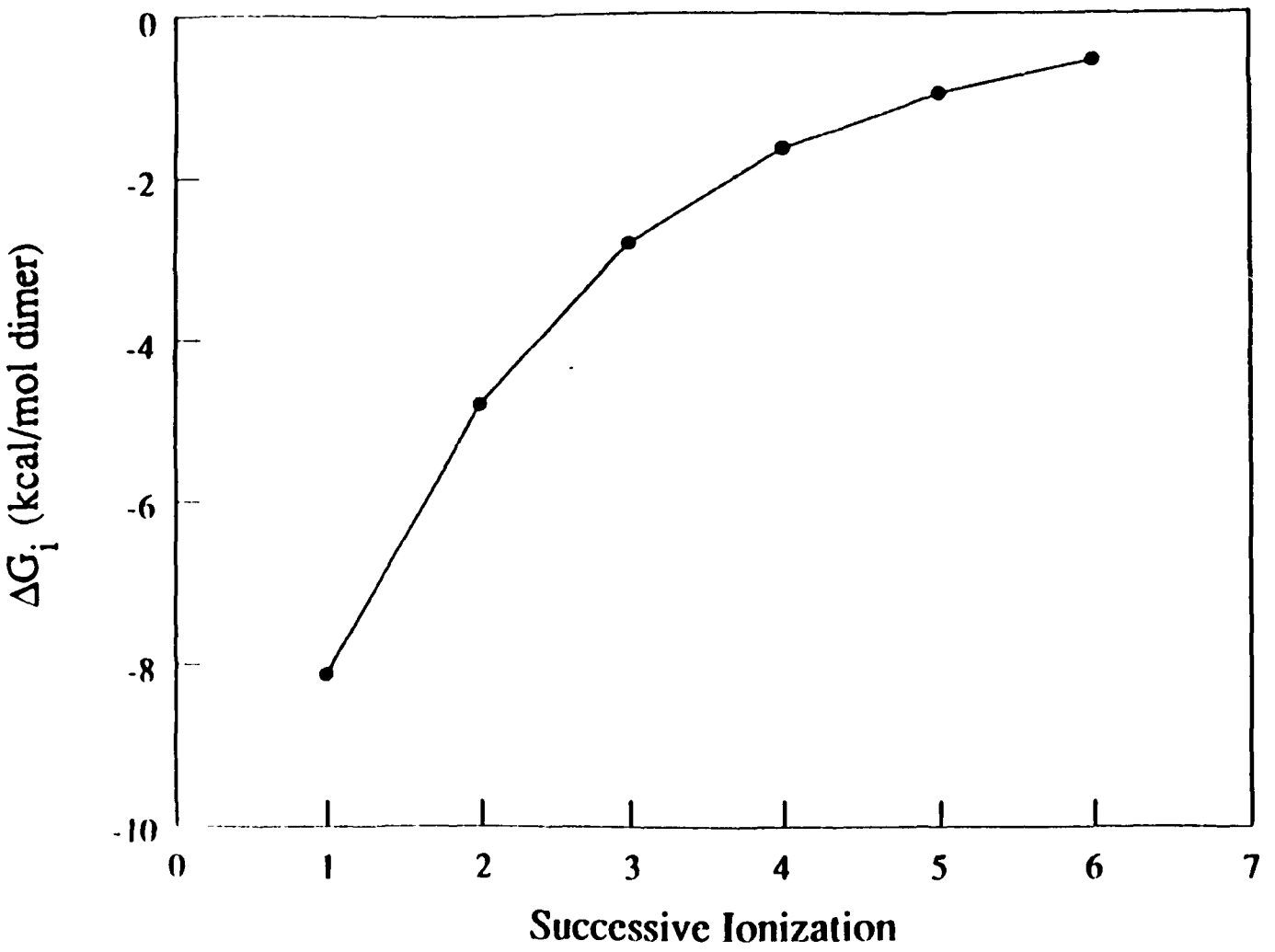
0
-2
-4
-6
-8
-10
ΔG_i (kcal/mol dimer)
0
1
2
3
4
5
6
7
Successive Ionization

Figure 5

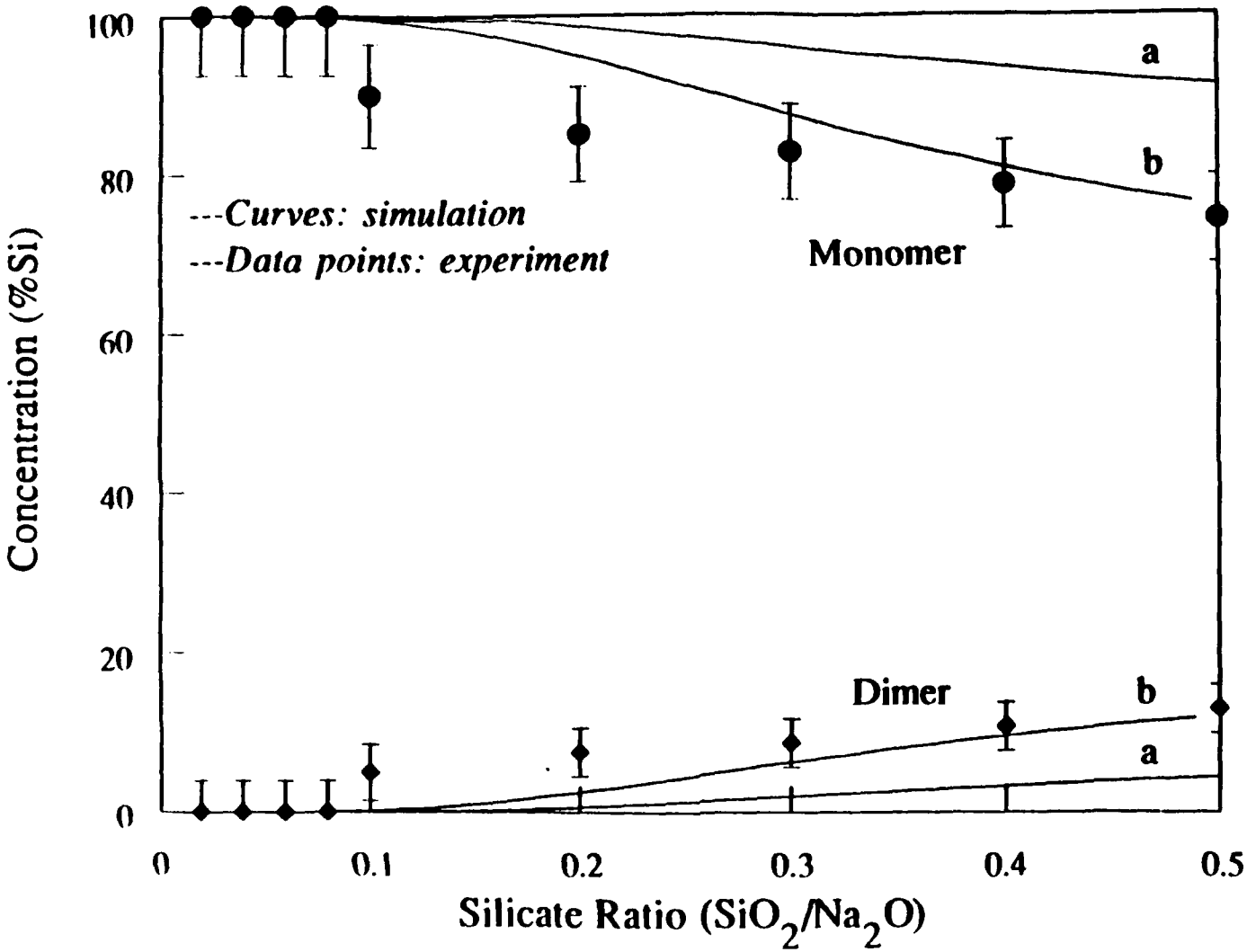
100
80
60
40
20
0
Concentration (%Si)
---Curves: simulation
---Data points: experiment
Monomer
a
b
Dimer
b
a
0
0.1
0.2
0.3
0.4
0.5
Silicate Ratio (SiO_2/Na_2O)

Figure 6

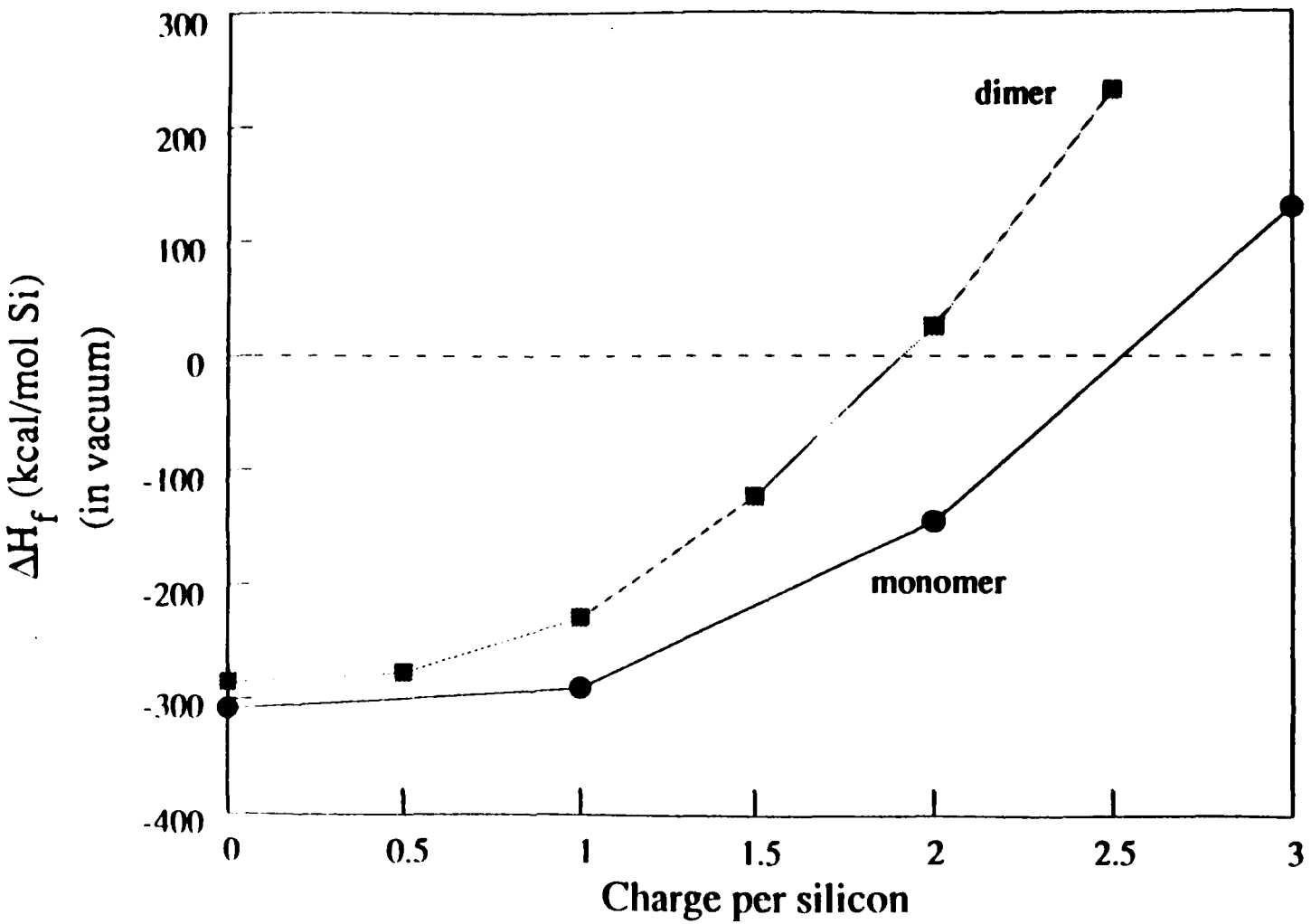
300
200
100
0
-100
-200
-300
-400
0
0.5
1
1.5
2
2.5
3
dimer
monomer
ΔH_f (kcal/mol Si)
(in vacuum)
Charge per silicon

Figure 7

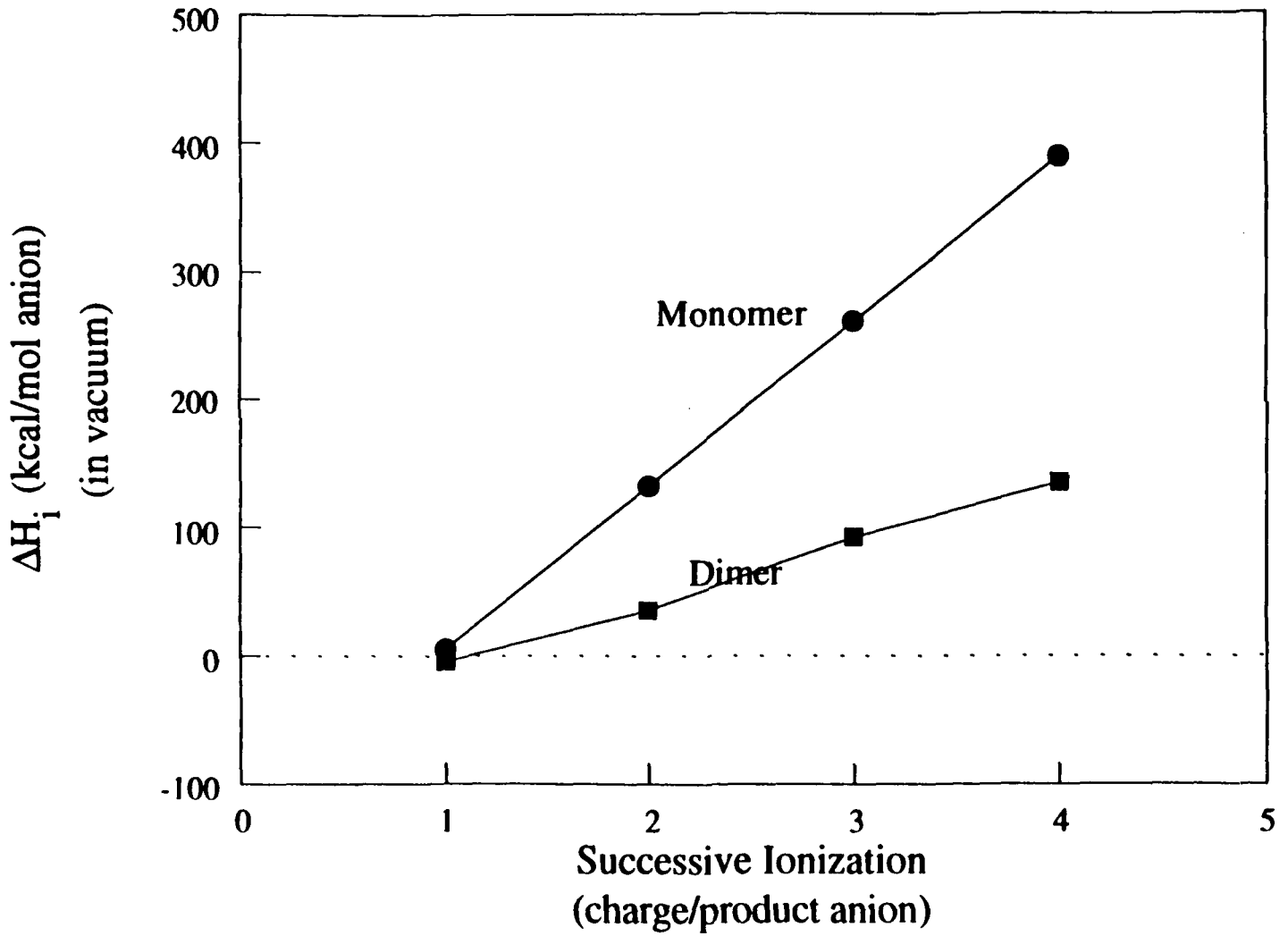
500
400
300
200
100
0
-100
0
1
2
3
4
5
Monomer
Dimer
ΔH_i (kcal/mol anion)
(in vacuum)
Successive Ionization
(charge/product anion)

Figure 8

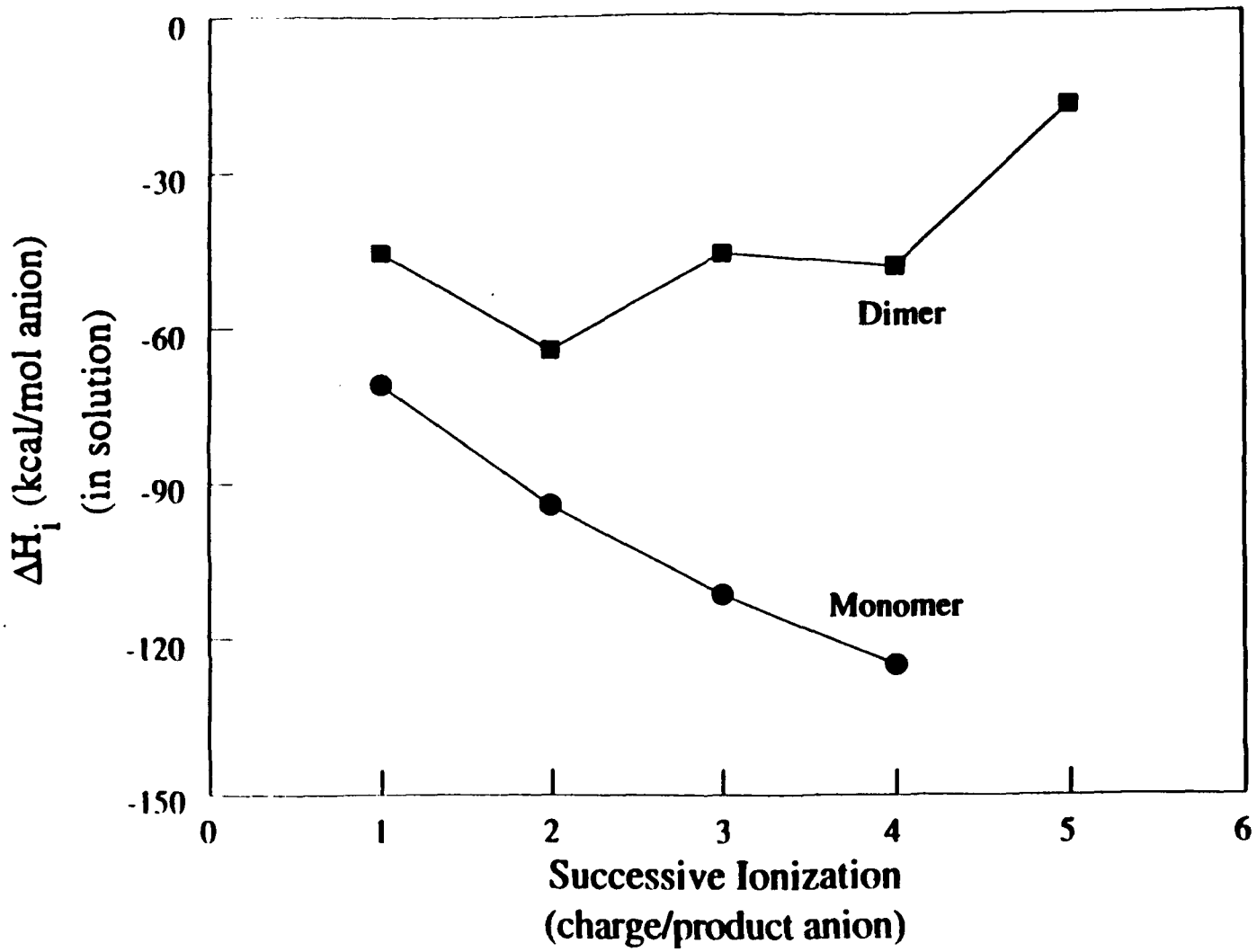
0
-30
-60
-90
-120
-150
ΔH_i (kcal/mol anion)
(in solution)
Dimer
Monomer
0
1
2
3
4
5
6
Successive Ionization
(charge/product anion)

Figure 9

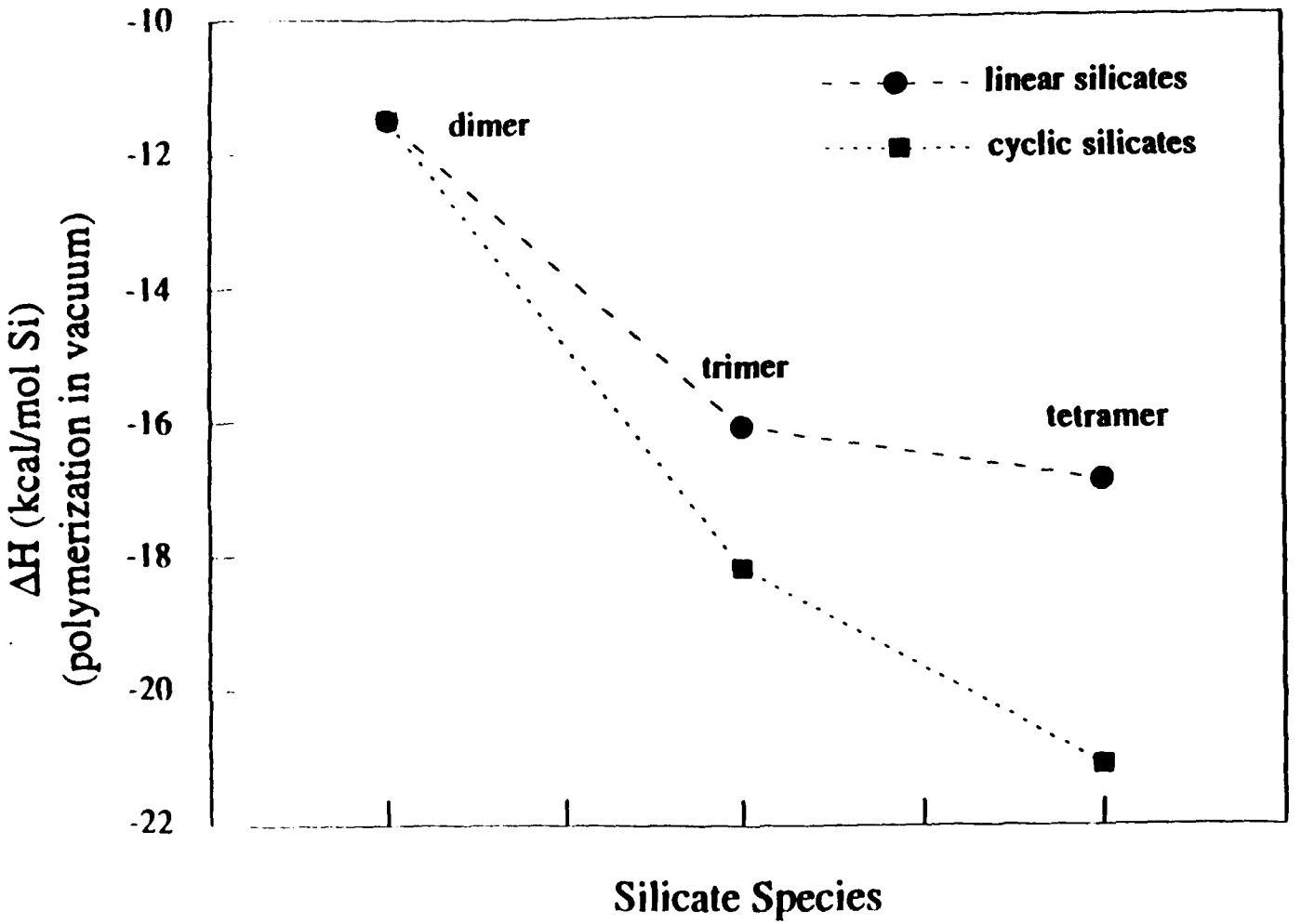
-10
-12
-14
-16
-18
-20
-22
ΔH (kcal/mol Si)
(polymerization in vacuum)
linear silicates
cyclic silicates
dimer
trimer
tetramer
Silicate Species

Figure 10

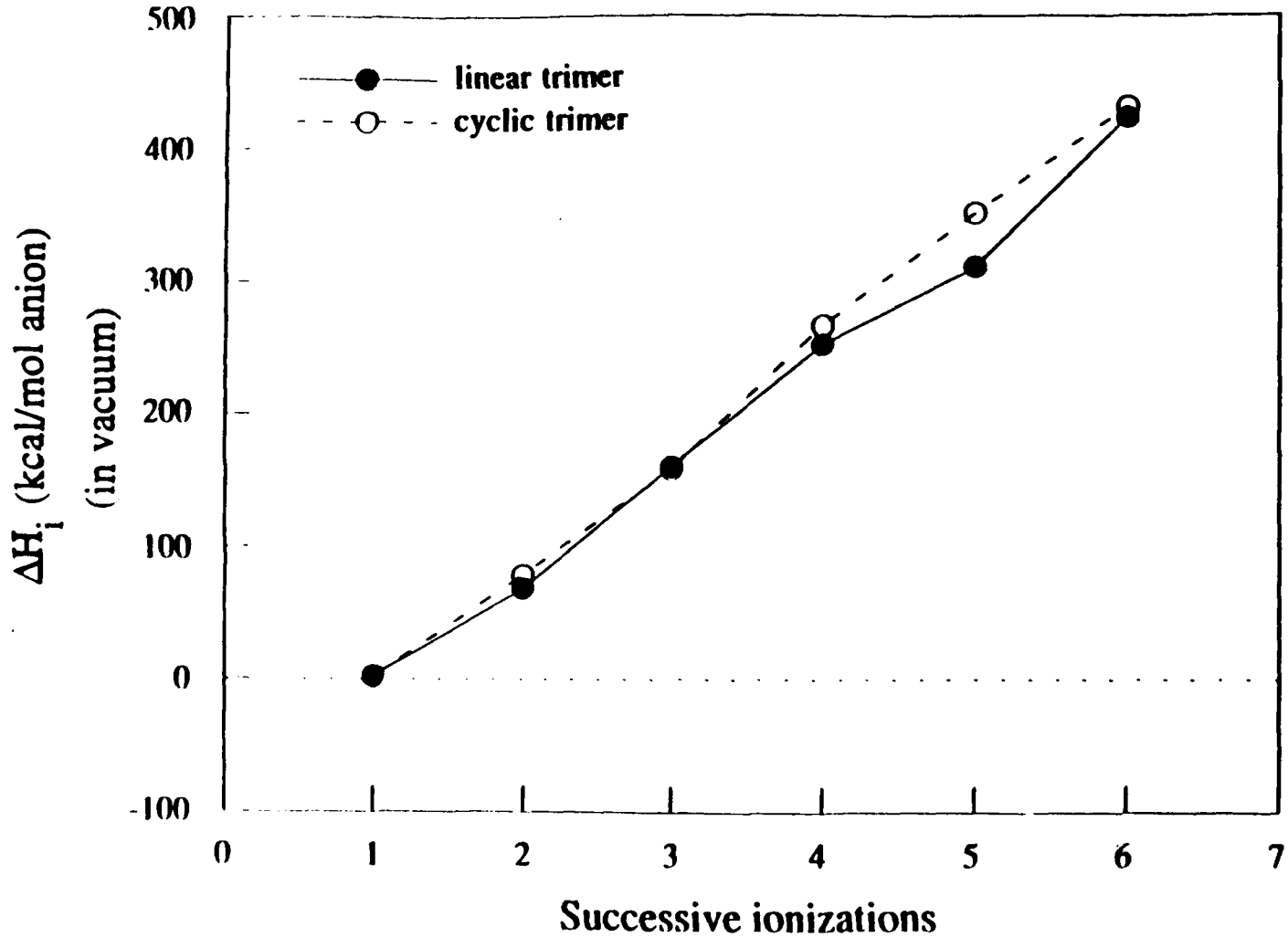
500
400
300
200
100
0
-100
0
1
2
3
4
5
6
7
linear trimer
cyclic trimer
ΔH_i (kcal/mol anion)
(in vacuum)
Successive ionizations

Figure 11

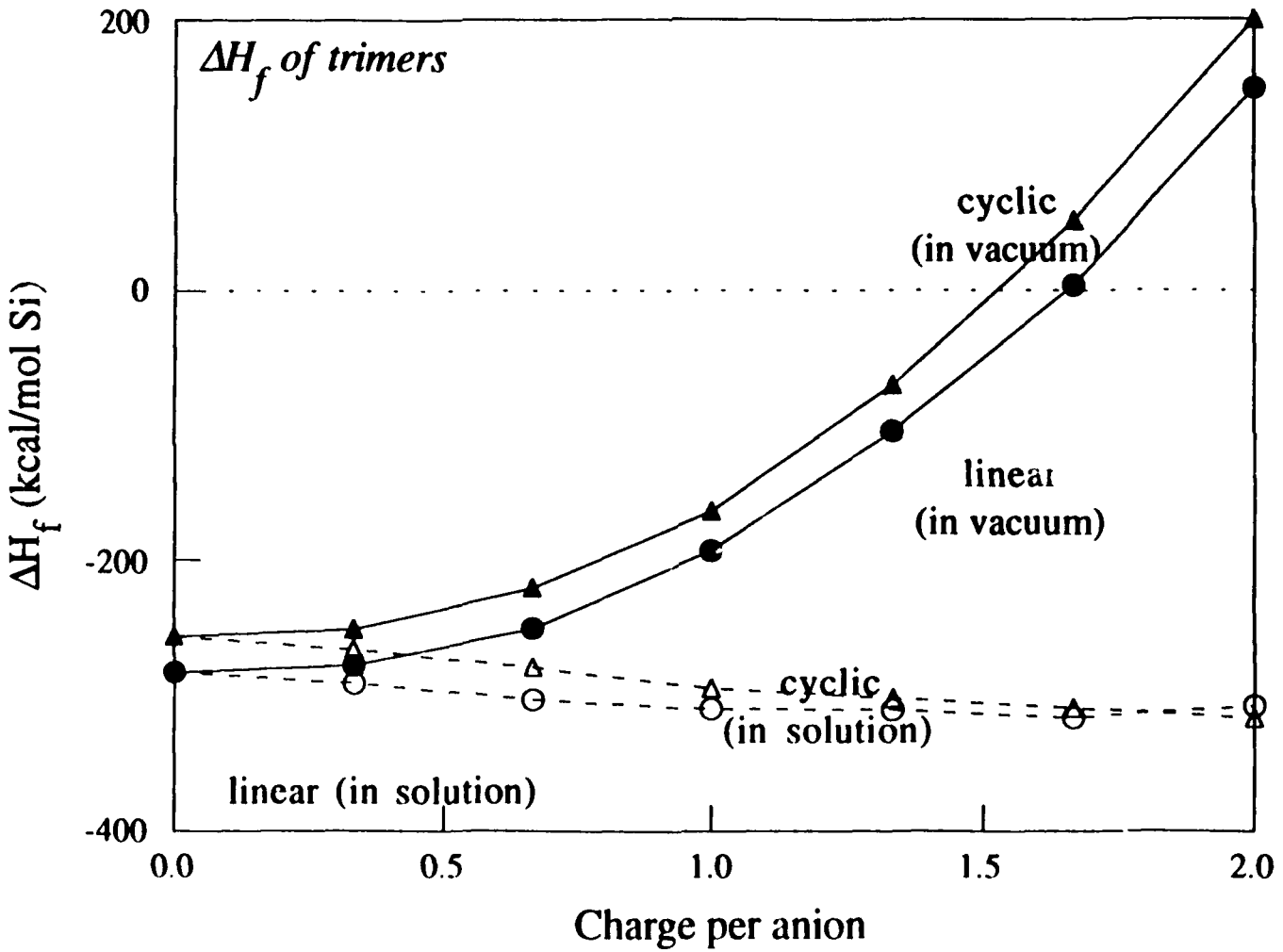
ΔH_f of trimers
200
0
-200
-400
ΔH_f (kcal/mol Si)
cyclic
(in vacuum)
linear
(in vacuum)
cyclic
(in solution)
linear (in solution)
0.0
0.5
1.0
1.5
2.0
Charge per anion

Figure 12

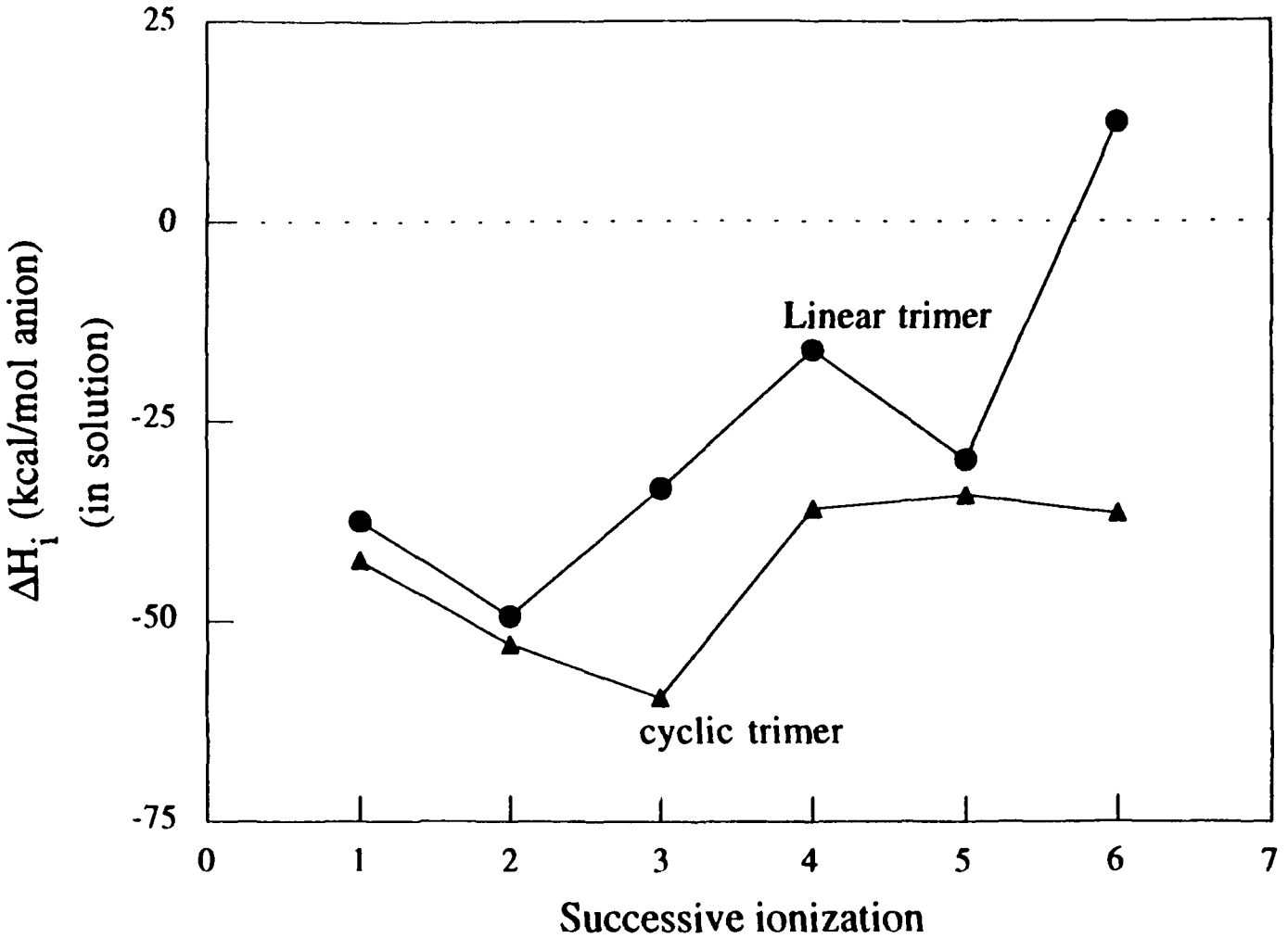
25
0
-25
-50
-75
ΔH_i (kcal/mol anion)
(in solution)
Linear trimer
cyclic trimer
0
1
2
3
4
5
6
7
Successive ionization

Figure 13

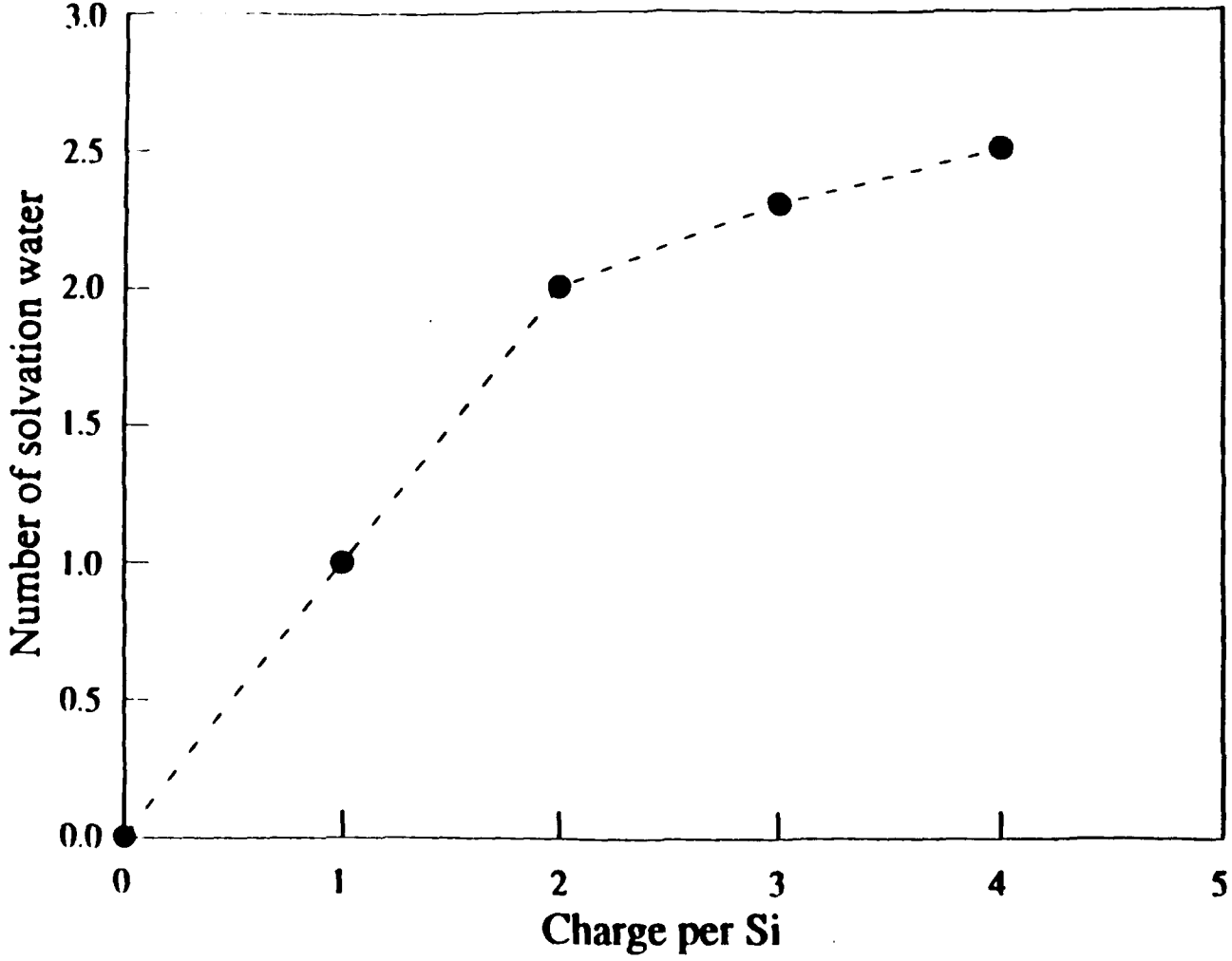
3.0
2.5
2.0
1.5
1.0
0.5
0.0
Number of solvation water
0
1
2
3
4
5
Charge per Si

Figure 14

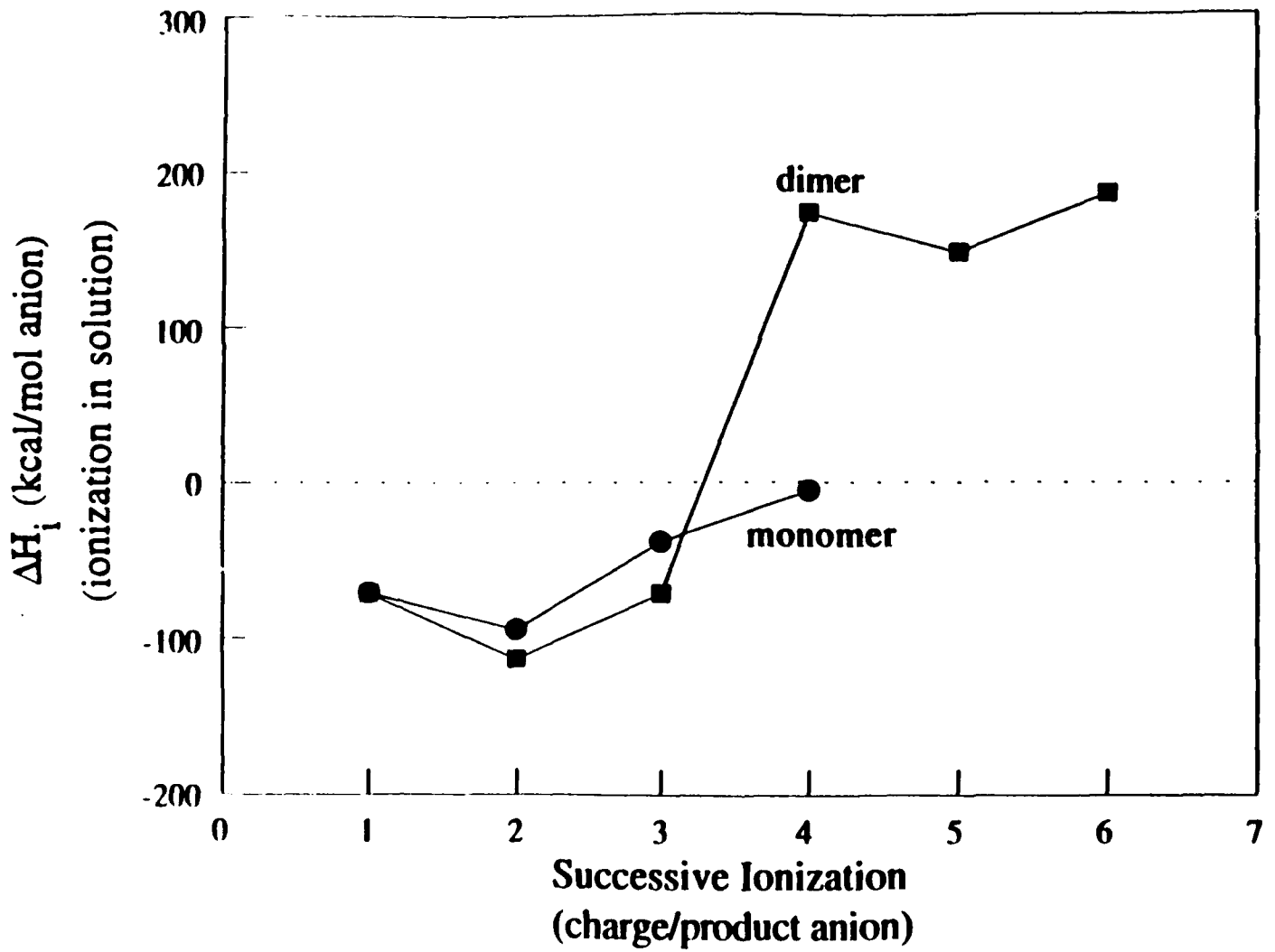
300
200
100
0
-100
-200
0
1
2
3
4
5
6
7
dimer
monomer
ΔH_i (kcal/mol anion)
(ionization in solution)
Successive Ionization
(charge/product anion)

Figure 15

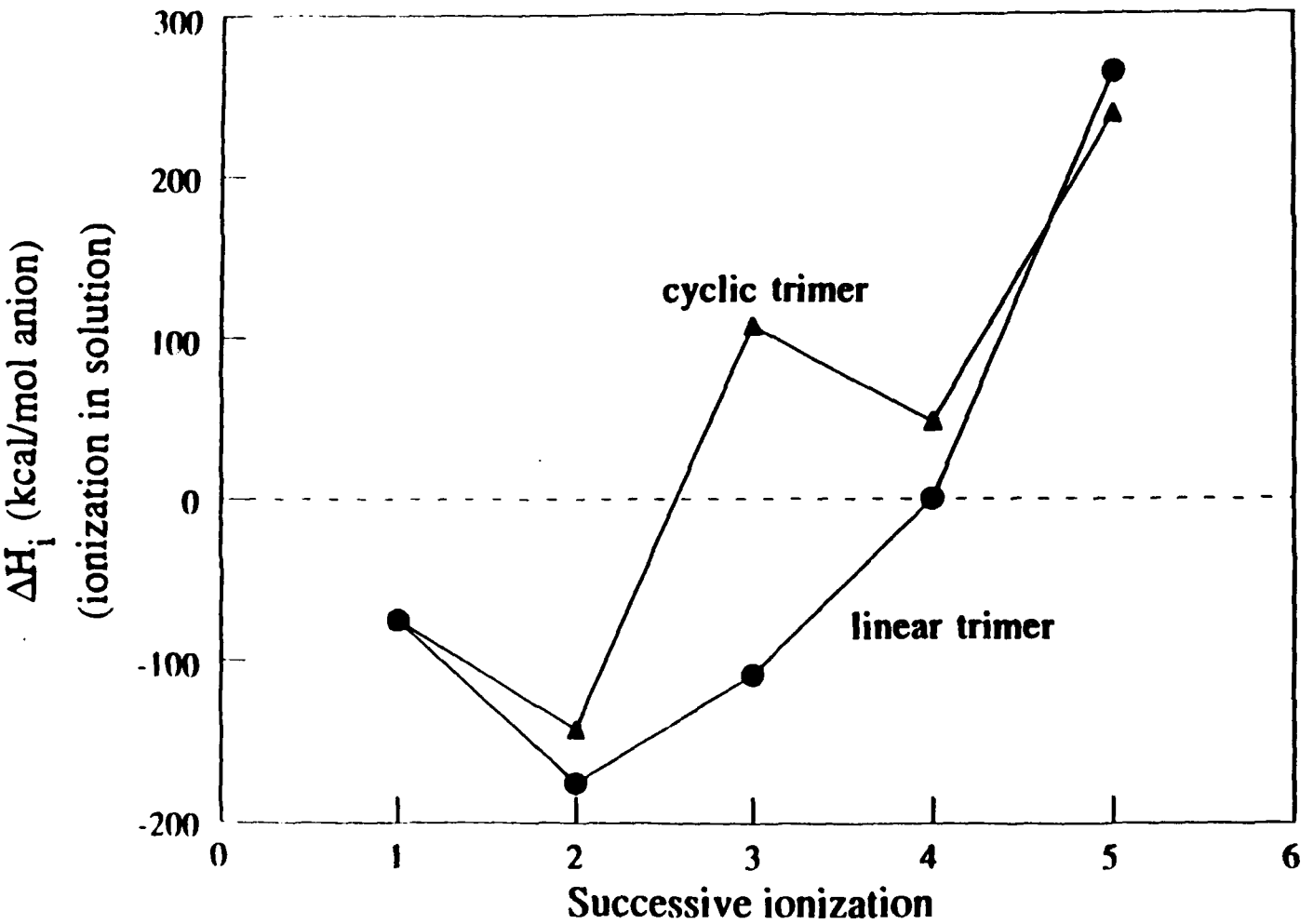
300
200
100
0
-100
-200
0
1
2
3
4
5
6
cyclic trimer
linear trimer
ΔH_i (kcal/mol anion)
(ionization in solution)
Successive ionization

Figure 16

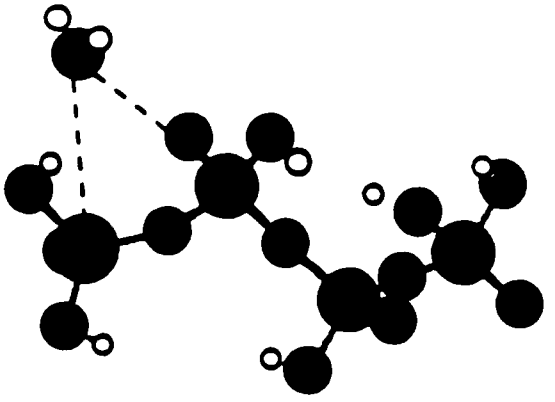

- a -

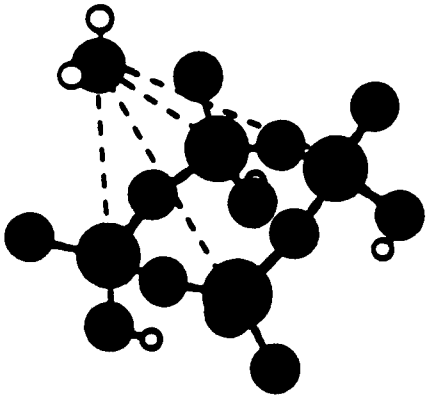

- b -

● - Silicon ● - Oxygen ○ - Hydrogen